Spring 2019

Modeling overpressure development during shale rock compaction coupling poroelasticity and permeability evolution above 3km depth

Wenyu Zhao

Department:

MODELING OVERPRESSURE DEVELOPMENT DURING SHALE ROCK COMPACTION COUPLING POROELASTICITY AND PERMEABILITY EVOLUTION ABOVE 3KM DEPTH

by

WENYU ZHAO

A THESIS

Presented to the Faculty of the Graduate School of

MISSOURI UNIVERSITY OF SCIENCE AND TECHNOLOGY

In Partial Fulfillment of the Requirements for the Degree

MASTER OF SCIENCE IN PETROLEUM ENGINEERING

2019

Approved by:

Andreas Eckert, Advisor
Mingzhen Wei
Jonathan Obrist Farner

ABSTRACT

The evolution of pore pressure including overpressure during sedimentation is an important process to consider when analyzing whether high pore pressure causes rock failure. High pore pressure is caused by under-compaction due to the rapid burial of low-permeability sediments, and as a result, porosity decreases less rapidly with depth than in normally compacted sediments where porosity decreases exponentially with depth. While under-compaction related pore pressure magnitudes have been determined empirically, in most numerical modeling approaches, the pore pressure is either applied as a static magnitude or coupled to a fluid flow simulator. This study simulates the pore pressure evolution during sediment loading and compaction using 3D porous-elastic-plastic finite element analysis. Continuous sedimentary loading is applied, and the resulting compaction process is coupled to the evolution of Poisson ratio and bulk modulus. The models test compacted sandstone and shale beds with varying ranges of physical properties including porosity, permeability, and elasticity for various sedimentation rates and initial physical properties distributions. Initial results show that overpressure occurs in rock layers with a permeability lower than 10^{-12} m^2 when the sedimentation rate is equal to or exceeds 10 mm/year. It also shows that porosity tends to either decrease much slower or temporarily stops decreasing with the development of overpressure. Porous space is easier to be compacted in rocks featuring a lower bulk modulus under the same effective stress. The presented procedure enables to couple the simulation of the effective state of stress both due to the initial burial history of a sedimentary basin therefore provides a better assessment for rock failure analysis.

ACKNOWLEDGMENTS

I would like to thank my advisor, Dr. Andreas Eckert, for giving me the chance to work in the Numerical Geomechanics Research Group. He was an excellent professor and mentor, and has contributed to my intellectual and personal development. His technical writing guidance was important to the development of this work. My gratitude to my committee members, Dr. Wei and Dr. Obrist Farner, helped me to improve my presentation skills and guide my research.

TABLE OF CONTENTS

Page

LIST OF ILLUSTRATIONS

LIST OF TABLES

1. INTRODUCTION

1.1. LITERATURE REVIEW

In order to understand porosity development mechanisms, experimental method, numerical modeling, and field measurement are three main approaches. Bjørlykke and Høeg (1996) investigates the influence of stress, compaction and fluid flow to burial diagenesis in sedimentary basins. According to their works, rock physical properties such as elastic properties (including Young's modulus, Poisson's ratio, and Bulk modulus), minerology, effective stress state, temperature, and fluid flow can affect porosity evolution. Physical compaction is the dominant mechanism controls porosity evolution above 3km because temperature is not high enough to cause smectite-illite transformation and/or hydrocarbon generation (i.e. chemical compaction). In oil industries, mechanical compaction is commonly considered as a principal fact affecting porosity evolution during sedimentary basin forming because experimental method and numerical modeling can reproduce rock physical compaction well and the major productive reservoirs are located above 3km depth (references). Zhang (2013) introduced a modified empirical equation based on Athy's equation and field observations. His work indicates the role of pore pressure in porosity prediction and shows that the development of overpressure decreases effective stress and leads to constant or enlargement of porous space. The modified Athy's equation considers effective stress as the most important parameter affecting porosity evolution and the magnitude of effective stress is controlled by overburden load and pore pressure. It improves the accuracy of porosity prediction in under-compacted reservoirs, but pore pressure and stress state are introduced as a constant boundary condition measured from well logging or estimated based on empirical equations. The pore pressure and stress

state estimation are the primary method rather than well logging measurement because it is convenient and relatively accurate. Lots of works investigated sedimentary basin modeling method and introduce estimated pore pressure and stress state as the initial conditions and obtain reservoir conditions. Though these studies gain relative good reproduce of sedimentary basin models, it cannot reproduce overpressure evolution dynamically, in the other word, the porosity evolution trend is not related with the effective stress state.

Several researches discuss the mechanism of overpressure development. Zhao (2018) summarizes that "The causes of overpressure are divided into five categories, namely, disequilibrium compaction, fluid expansion, diagenesis, tectonic compression and pressure transfer." When the temperature does not reach the oil window, compaction disequilibrium is considered as the dominant mechanism generating overpressure above 3km depth. For such conditions, consolidation is mainly controlled by the process of mechanical compaction (Bjørlykke and Høeg, 1996). Overpressure caused by compaction disequilibrium is usually observed in clay-rich sandstone and shale rock because of their low permeability (e.g. 1 x 10-6 mD) (Revil and Cathles, 1999). Chemical compaction results from diagenesis as permeability decrease during the smectite-illite transformation resulting overpressure. Fluid expansion can be classified into hydrocarbon generation, gas generation, and thermal expansion (Zhao, 2018). Since diagenesis and fluid expansion are significantly controlled by temperature, chemical compaction is not considered as a dominant mechanic causing overpressure above 3km, where temperature is not high enough (Bjørlykke and Høeg, 1996).

Experimental studies and analytical models on mechanical compaction indicate that porosity has an empirical relationship with the elastic properties (i.e. Young's modulus E, Bulk modulus K, and Poisson's ratio υ), permeability, and pore pressure within the same type of rock (Mesri and Olson, 1971; Vernik et al., 1993; Vasseur et al., 1995; Revil and Cathles 1999; Goulty, 1998; Chang et al., 2006; Mondol et al., 2007; Yang and Aplin, 2010; Zhang, 2013; Zhang et al., 2015). Many experimental studies have investigated mechanical compaction by compacting rock samples or artifacts (e.g. smectite-kaolinite mixture) to quantify porosity-elastic properties relationships (Vernik et al., 1993; Vasseur et al., 1995; Goulty, 1998; Chang et al., 2006; Mondol et al., 2007). Chang et al. (2006) used 100 shale samples to calibrate relationships among Young's modulus, porosity and uniaxial compressional strength (UCS). Their study shows that porosity decreases when UCS increases, and E is enhanced when the rock has a larger UCS. Many studies have focused on the porosity-permeability relationship of shale rock (Mesri and Olson, 1971; Yang and Aplin, 2010; Zhang et al., 2015). Mesri and Olson (1971) investigate how grain shape and size, and porosity influence the permeability of shale rock. Their study indicates that a fully saturated shale rock composed of fine and small grains (e.g. Smectite) has relatively low permeability, and the nonpolar pore fluid can flow relatively easier in the same rock (e.g., Benzene).

Overpressure is a key parameter controlling effective stress, and porosity-pore pressure relationships are usually discussed through porosity-effective stress relationships. According to field data, depending on the development gradient of pore pressure, porosity can keep constant or increase with depth when pore pressure gradient equals or larger than overburden gradient (Revil and Cathles 1999; Zhang, 2013). The sedimentary basin

compaction geomechanical models coupled with development of normal stress state is well development. To eliminate the gravity influence, geomechanical models are pre-stressed. However, the overpressure development cannot be simulated by using these models because the permeability is a constant initial condition assigned into models. According to these published studies, the experimental method can observe and measure porosity and elastic properties directly and estimate permeability from porosity. The mechanical compaction of shale rock can be explained by composing these studies theoretically, but it is difficult to be investigated by using the experimental method. Moreover, simulating shale rock consolidation associated with overpressure and rock properties development in a real geological time scale is quite impossible through experimental method. To eliminate this problem, this study simulates shale rock consolidation associated with pore pressure development during sediment loading and compaction above 3km depth, using 3D porous-elastic-plastic finite element analysis. Continuous sedimentary loading is applied, and the resulting compaction process is coupled with the evolution of Poisson's ratio, bulk modulus, and permeability. The model test compacted shale rock with varying ranges of physical properties including porosity, permeability, and elastic properties for various sedimentation rates and initial physical properties distributions. Field data from North Sea shale and the Minibasin of Gulf of Mexico are reproduced.

1.2. RESEARCH OBJECTIVES AND QUESTIONS

Knowledge of the in-situ effective state of stress is of crucial significance during the generation of mechanical earth models (MEM) of sedimentary basins in order to provide information for drilling management, well stability, fracture design, and reservoir evaluation (Zoback et al., 1985; Moos and Zoback, 1990; Mclean and Addis, 1991; Hossain et al., 2000;

Plumb et al., 2000). Obtaining the total in-situ stress magnitudes for a MEM is based on well-established methods involving: (1) measurement of the vertical stress based on the integrated well log (Karahara, 1966); (2) measurement of the minimum horizontal stress based on mini fracture tests (Bell,1990); (3) estimation based on dynamic elastic properties in a MEM with or without accounting for tectonic & thermal contributions (Prats and Maraven, 1989; Warpinski, 1989; Thiercelin and Plumb, 1994; Blanton and Olson, 1999; Mcdermott and Kolditz, 2006; Zoback, 2007). For basins with complex subsurface geology & complex material property distributions, numerical approaches such as 3D finite element analysis are used. Such numerical models involve a pre-stressing step to account for gravitational equilibrium (e.g. Eckert and Liu, 2014) and application of traction boundary conditions (Steckler and Watts, 1978; Sclater and Christie, 1980; Becker et al., 2010). Pore pressure is commonly introduced as a static value derived from production data or physical measurements (e.g. repeat formation test). However, for low permeability rocks, direct pore pressure measurements or production data are usually not available (Sclater and Christie, 1980; Plumb et al., 2000; Becker et al., 2010), yet the increased likelihood of overpressure below 2 km (Zhang, 2011) highlights the necessity of its accurate inclusion in MEMs. Under consistent total state of stress conditions, effective stress decrease due to overpressure development can improve the possibility of rock failure (Cosgrove, 1997; Mcdermott and Kolditz, 2006; Olson, 2008). The porosity of rock can decrease slower than the one under normal compaction condition, remain constant, or increase depending on the degree of overpressure development (Revil and Cathles, 2002; Zhang, 2011; Zhang, 2013). For overpressure and porosity prediction, in the absence of physical measurements, porosity and pore pressure are estimated through empirical relationships (e.g. Athy's equation and depth equivalent method). By using

this approach, pore pressure and porosity are introduced into numerical models as initial boundary conditions. However, these empirical relationships do not account for the coupling of pore pressure to the poroelastic compaction process, and thus modeling results are not able to predict the effective stress appropriately throughout the sedimentary basin burial process.

To overcome this problem, MEMs based on a finite element the associated modeling approach simulating sedimentary rock consolidation and pore pressure evolution are developed. The modeling approach enables to simulate the effective state of stress in low permeability rocks and accounts for the development of overpressure throughout the burial history of the basins. Zhao (2018) summarizes that "The causes of overpressure are divided into five categories, namely, compaction disequilibrium, fluid expansion, diagenesis, tectonic compression and pressure transfer." When the temperature does not reach the oil window, compaction disequilibrium is considered as the dominant mechanism generating overpressure (i.e.above 3km depth) (Bjørlykke and Høeg, 1996). For such conditions, consolidation is mainly controlled by the process of mechanical compaction (Bjørlykke and Høeg, 1996). Overpressure caused by compaction disequilibrium is usually observed in clay-rich sandstone and shale rock because of their low permeability (e.g. 1 x 10-20 m^2) (Revil and Cathles, 1999). Chemical compaction results from diagenesis as permeability decreases during the smectite-illite transformation resulting in overpressure. Fluid expansion can be classified into hydrocarbon generation, gas generation, and thermal expansion (Zhao, 2018).

Since diagenesis and fluid expansion are significantly controlled by temperature, chemical compaction is not considered as a dominant mechanism causing overpressure above 3km, where temperature is not high enough (Bjørlykke and Høeg, 1996). Experimental studies and analytical models on mechanical compaction indicate that porosity is related to elastic

properties (i.e. Young's modulus E, Bulk modulus K, and Poisson's ratio υ), permeability, and pore pressure (Mesri and Olson, 1971; Vernik et al., 1993; Vasseur et al., 1995; Revil and Cathles 1999; Goulty, 1998; Chang et al., 2006; Mondol et al., 2007; Yang and Aplin, 2010; Zhang, 2013; Zhang et al., 2015). Many experimental studies investigated mechanical compaction by compacting samples to quantify porosity-elastic property relationships (Vernik et al., 1993; Vasseur et al., 1995; Goulty, 1998; Chang et al., 2006; Mondol et al., 2007). Chang et al. (2006) show that porosity decreases when uniaxial compressional strength (UCS) increases, and the Young's modulus is enhanced when the rock has a larger UCS. Many studies have also focused on the porosity-permeability relationship of shale rock (Mesri and Olson, 1971; Yang and Aplin, 2010; Zhang et al., 2015). Mesri and Olson (1971) observed that a fully saturated shale rock composed of fine and small grains (e.g. Smectite) has relatively low permeability, and the nonpolar pore fluid can flow relatively easier in the same rock (e.g. Benzene).

Though empirical relationships (i.e. Athy's equation) can estimate pore pressure and porosity relatively accurate but not provide the inter-relationships among pore pressure, porosity, permeability, rock elastic properties, and effective state of stress. As a result, this method cannot provide acceptable estimations for every sedimentary basin (e.g. porosity evolution of the North Sea shale rock (Chang, 2006). This study develops a consistent geomechanical modeling procedure based on 2D/3D finite element analysis that is capable to simulate the development of overpressure and the relation to the evolving porosity and shale rock elastic-plastic properties distribution. Following the experiment results, rock properties including permeability, elastic properties development are coupling with the evolution of porosity during compaction through ABAQUS^{TM} subroutine.

2. METHODOLOGY

2.1. GOVERNING EQUATIONS

The modified Cam-Clay Model (MCCM) associated rock elastic properties and permeability evolution is used in this study to simulate a layer of shale rock consolidation from surface to 2-3km depth and two case studies: (1) North Sea shale rock porosity-effective vertical stress relationship; (2) The Minibasin well profile at the Gulf of Mexico. MCCM is an elastic-plastic strain hardening model describing relationships between the logarithmic mean effective stress, *p'*, and the specific volume, *v* (Figure 2.1).

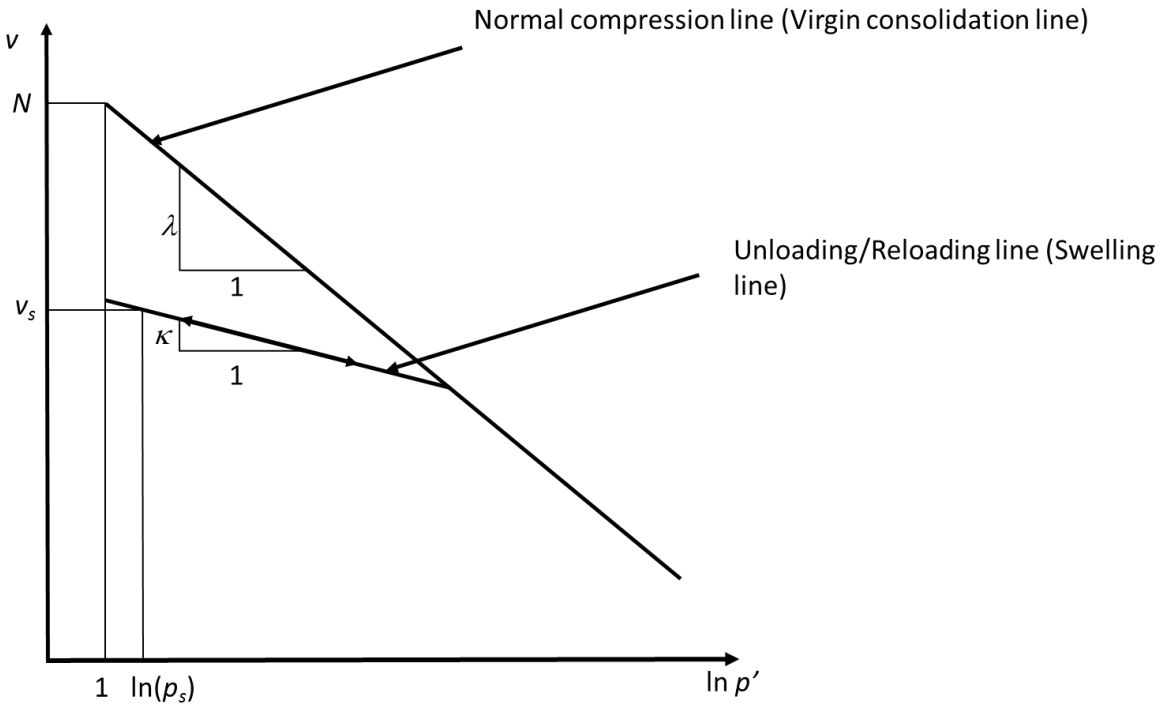

Figure 2.1. The relationship between specific volume and effective stress.

The MCCM model compressional lines are defined by the following equations:

$$v = N - \lambda \ln(p')$$

$$v = v_s - \kappa \ln(p_s)$$

$$v = 1 + e$$

$$e = \phi/(1 - \phi)$$

λ is the slope of the normal compression line and κ is the slope of swelling line (reloading/unloading line). *N* is defined as the specific volume of normal compression line when logarithmic mean stress is 1. v_s is the specific volume and p_s is the specific mean effective stress during reloading/unloading process. *e* is the void ratio and ϕ is the porosity. These parameters are essential properties for shale rock simulation. In this study, the normal compression line refers to the shale rock normal consolidation process with hydrostatic pore pressure development and the swelling line represents overpressure developing and equilibrating process.

According to other studies such as Bjørlykke and Høeg (1996) and Allen and Allen (2013), this model can reproduce normal consolidation process and overpressure development through the relationship between effective stress and porosity. Bjørlykke and Høeg (1996) introduce the behavior of normal consolidation of sediments (Figure 2.2). It shows the relationship between vertical effective stress σ_v' and vertical compression ε_v' using the same principle to describe normal consolidation process. Allen and Allen (2013) also show the result of a 1-D compression normal consolidation test (i.e. Modified Cam-Clay Model) which illustrates the relationship between void ratio and effective vertical stress. Their observation indicates the ability of MCCM on simulating rock consolidation.

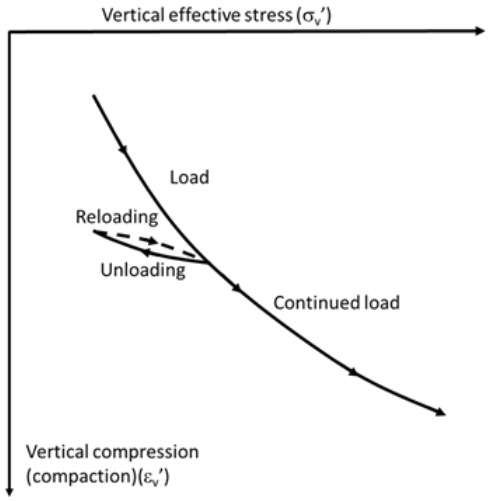

Figure 2.2. Sedimentary rock consolidation mechanism following Bjørlykke and Høeg (1996) work.

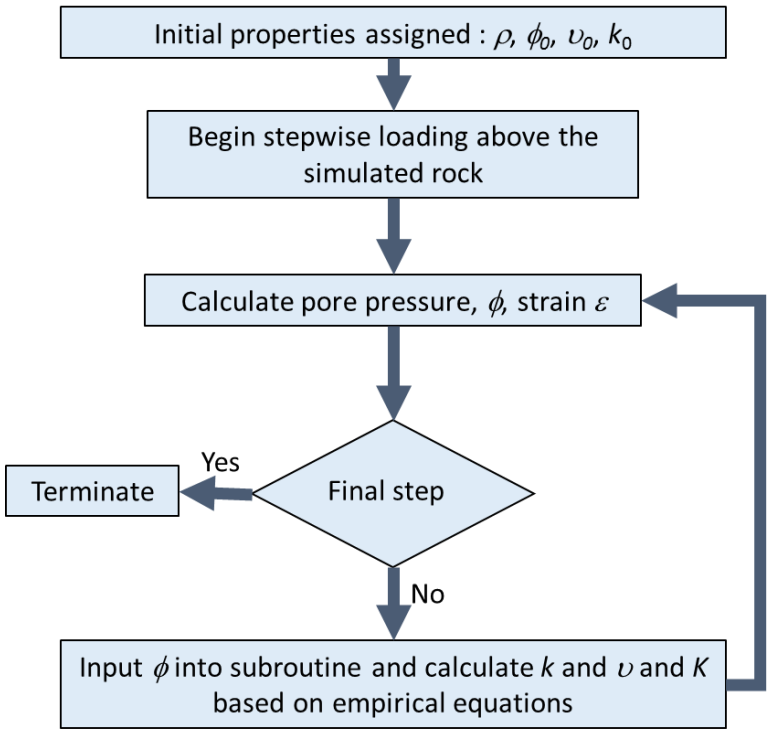

Figure 2.3. The flow chart of using subroutine in this numerical modeling study.

2.2. SUBROUTINE APPLICATION

In this study, the evolution of rock elastic properties and permeability is coupled into the MCCM by using ABAQUS™ subroutine (Figure 2.3). This shale rock layer is compacted by sediments accumulated above it and subsidizing from surface to 3km depth through 2 million years. By the end of each increment (i.e. 30m thick sediments accommodation), the rock properties (i.e. elastic properties and permeability) are updated through subroutine according to the current effective stress and porosity. This coupling process means to generate a better numerical reproduce of consolidation and overpressure development because most of the time permeability and elastic properties are assigned into numerical models as constant boundary conditions. The rock property evolution trends are based on experimental results. Mondol et al. (2007) investigate the relationship between Poisson's ratio and vertical effective stress by compacting samples composed of varying friction of smectite-kaolinite (Figure 2.4). An interpreted equation used in the subroutine to represent the evolution of Poisson's ratio is

$$\upsilon = \upsilon_{min} + (0.5 - \upsilon_{min})e^{-0.3\sigma_{v}'}$$

$$K = -vp'/\kappa$$

$$v = v_s - \kappa \ln(p_s)$$

$$v = N - \lambda \ln(p')$$

υ is the Poisson's ratio and υ_{min} is the minimum Poisson's ratio of this rock. σ_v' is the vertical effective stress. During simulation, bulk modulus, *K*, is calculated during simulation by specific volume, *v*, mean effective stress, *p'*, and the slope of swelling line, κ.

Mesri and Olson (1971) test porosity-permeability relationship by using rock samples composed of kaolinite, illite or smectite saturated with varying fluid types including water, water (NaCl), water ($CaCl_2$), Ethyl/Methyl Alcohol, and Benzene.

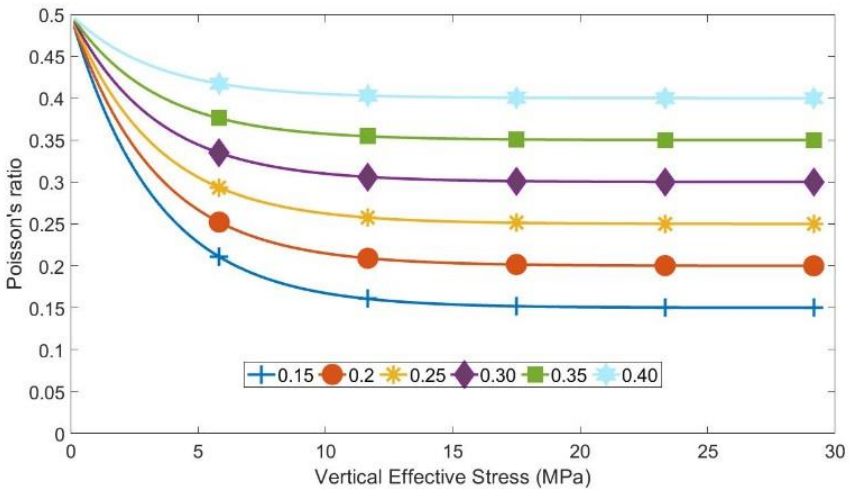

Figure 2.4. The relationship between Poisson's ratio and effective stress.

In this study, the shale rock is assumed it is fully saturated with sea water and is composed of pure kaolinite, pure smectite, or varying friction of kaolinite-smectite mixture. Following Revil and Cathles' work (1999), empirical porosity-permeability equations interpreted from Mesri and Olson experimental results are used during consolidation simulation (Table 2.1 and Figure 2.5). The model test compacted shale rock with varying ranges of physical properties including porosity, permeability, and elastic properties for various sedimentation rates and initial physical properties distributions.

$$k = k_0(\frac{\phi}{\phi_0})^{3m}$$

Table 2.1. The different constant numbers used for shale rock composed of kaolinite and smectite.

Shale	m	k_0 (ϕ_0=0.5), mD
kaolinite	2.34	7.1
smectite	4.17	3.1E-7

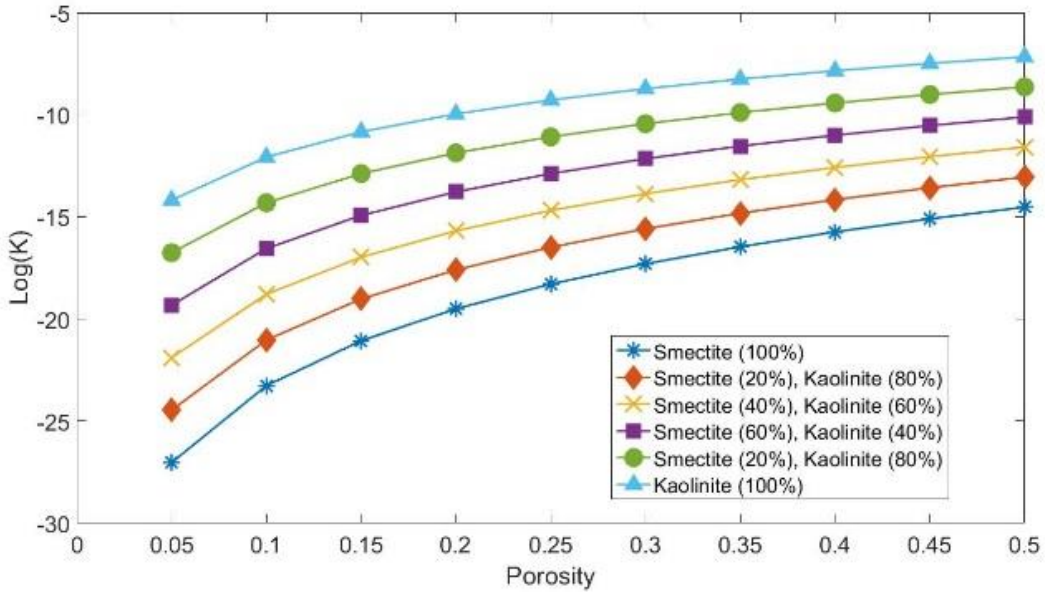

Figure 2.5. The evolution trend of porosity vs. permeability for different shale rock.

For theoretical analysis, a 40x10x10m shale rock layer composed of 4000 1x1x1m elements is simulated to reproduce the consolidation process from 0km to 2.5km depth (Figure 2.6).

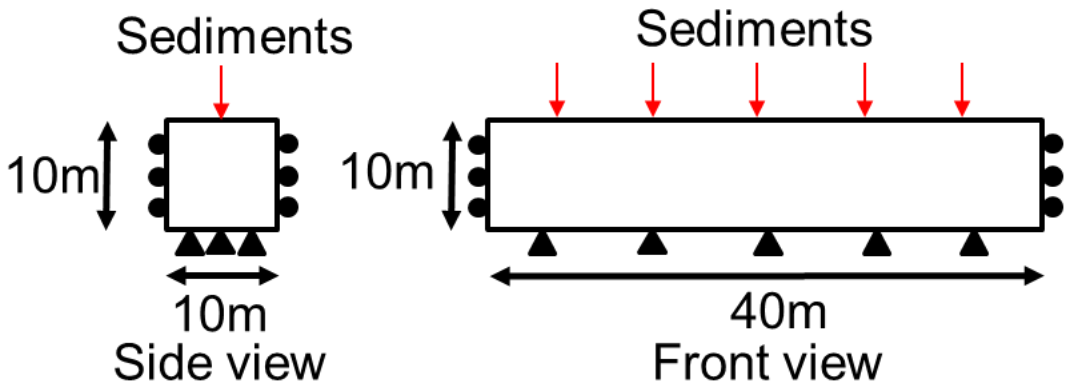

Figure 2.6. The numerical modeling setup.

This study has several significant assumptions: (1) The shale rock keeps subsidizing from surface to 3km depth through entire simulation and the depositional environment is always accommodation. (2) There is no shear deformation during the entire simulation. (3) Chemical compaction and thermal expansion are not considered. (4) The slope of the normal consolidation line is three times of unloading/reloading line. (5) The density of rock is 2265 kg/m^3 and initial porosity is 0.45. Table (2.2) shows the initial conditions and test scenarios, and the rock properties are based on core data from the Gulf of Mexico. Two case studies are discussed: (1) The MCCM is used to reproduce shale rock normal-compaction porosity development of North Sea following Chang's work (2006). (2) Porosity and pore pressure (including overpressure) of Minibasin is reproduced comparing with Revil and Cathles' work (1999). Tectonic is also considered as a parameter affecting porosity and pore pressure development, and it is introduced as a constant strain rate (10^{-14} ε/s).

Table 2.2. Material properties for this study. Scenario I is considering the influence of λ elastic properties; Scenario II is considering the influence of Poisson's ratio; Scenario III means to find how sedimentation rate and permeability affect overpressure development.

Scenairo I	Lamb (*l*)	Kapa (*k*)	Poisson's ratio(*u*)	sedimentation rate(m/m.a.)	permeability (m^2)
1	0.15	0.05	0.25	100	1.00E-11
2	0.2	0.067	0.25	100	1.00E-11
3	0.25	0.083	0.25	100	1.00E-11
4	0.3	0.1	0.25	100	1.00E-11
5	0.35	0.0117	0.25	100	1.00E-11
6	0.4	0.133	0.25	100	1.00E-11
7	0.45	0.15	0.25	100	1.00E-11
8	0.5	0.167	0.25	100	1.00E-11
Scenairo II	Lamb (*l*)	Kapa (*k*)	Poisson's ratio(*u*)	sedimentation rate(m/m.a.)	permeability (m^2)
1	0.4	0.133	0.15	100	1.00E-11
2	0.4	0.133	0.2	100	1.00E-11
3	0.4	0.133	0.25	100	1.00E-11
4	0.4	0.133	0.3	100	1.00E-11
5	0.4	0.133	0.5-0.2	100	1.00E-11
6	0.4	0.133	0.5-0.3	100	1.00E-11
7	0.4	0.133	0.5-0.4	100	1.00E-11
Scenario III	Lamb (*l*)	Kapa (*k*)	Poisson's ratio(*u*)	sedimentation rate(m/m.a.)	permeability (m^2)
1	0.4	0.13	0.25	2500	1.02E-20
2	0.4	0.13	0.25	2500	1.02E-21
3	0.4	0.13	0.25	2500	1.02E-22
4	0.4	0.13	0.25	3000	1.00E-20
5	0.4	0.13	0.25	4500	1.00E-20
6	0.4	0.13	0.25	6000	1.00E-20
7	0.45	0.2	0.5-0.2	1500	100%smectite
8	0.45	0.2	0.5-0.2	1500	20%kaolinite-80%smectite
9	0.45	0.2	0.5-0.2	1500	40%kaolinite-60%smectite
10	0.45	0.2	0.5-0.2	1500	60%kaolinite-40%smectite
11	0.45	0.2	0.5-0.2	1500	80%kaolinite-20%smectite
12	0.45	0.2	0.5-0.2	1500	100%kaolinite

This study simulates shale rock consolidation associated with pore pressure development during sediment loading and compaction above 3km depth, using 3D porous-elastic-plastic finite element analysis. Continuous sedimentary loading is applied, and the resulting compaction process is coupled with the evolution of Poisson's ratio, bulk modulus, and permeability. The model test compacted shale rock with varying ranges of physical properties including porosity, permeability, and elastic properties for various sedimentation rates and initial physical properties distributions. Field data from North Sea shale and the Minibasin of Gulf of Mexico are reproduced.

3. RESULTS

3.1. SENSITIVITY CHECK OF THE SLOPE OF NORMAL CONSOLIDATION LINE AND THE POISSON'S RATIO

If there are no overpressure development and uplifting during the entire simulation, this model undergoes a pure normal consolidation process. A constant Poisson's ratio 0.25 is assigned, and different bulk modulus magnitudes are tested by changing the slope of the normal consolidation line (Figure 3.1). The blue dashed line is the interpretation of the North Sea porosity following Chang's work (2006), and the red dashed line is the modified Athy's equation. The modified Athy's equation cannot reproduce the evolution of shale rock porosity of the North Sea. The result of MCCM yields the North Sea porosity profile when λ is 0.63 and κ is 0.21. The porous space of rock having a larger magnitude of λ can be reduced more under the same state of stress. The empirical equation from Chang (2006) is interpreted from the shale rock sample experimental result, and the Modified Athy's equation means to predict porosity below the sea floor. Both of them have less credibility on predicting porosity in shallow depth (e.g., 0-500m). In this study, an initial porosity 0.45 is assumed at the surface which can result in different initial porosity comparing with their empirical equations.

Bulk modulus is not only controlled by λ/κ but also related to the Poisson's ratio. To test how the Poisson's ratio affects modeling results, Figure 3.2 illustrates constant Poisson's ratio 0.15~0.40 are assigned into the model with λ=0.57 and κ=0.19. Rock has larger Poisson's ratio is easier to be compacted, and the differential porosity is increasing with depth. Rock having 0.40 Poisson's ratio yields the North Sea porosity closer, but it cannot match it as well as the one having λ=0.63, κ=0.21, and Poisson's ratio=0.25.

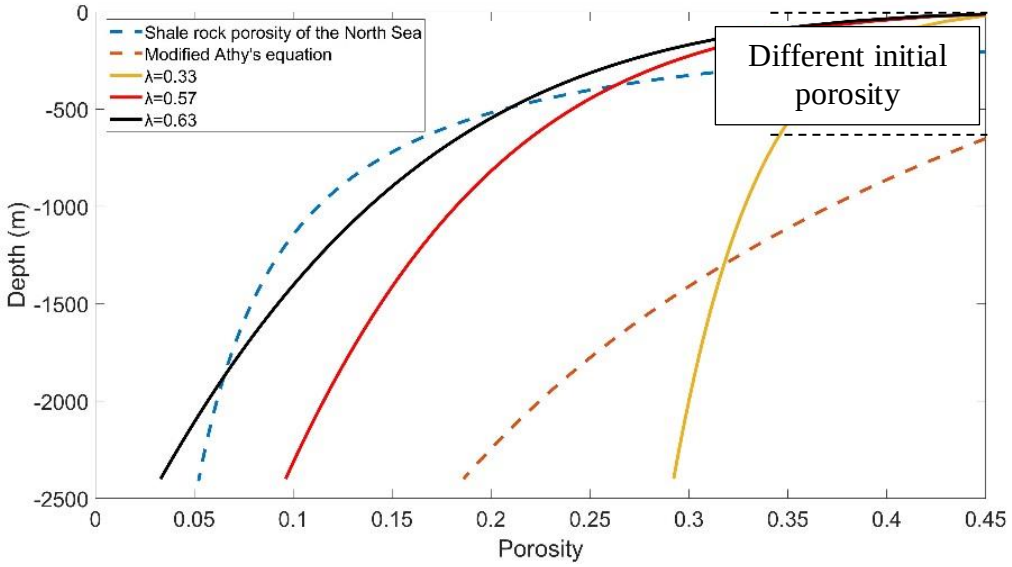

Figure 3.1. Sensitivity check of the slope of normal consolidation (λ). This figure shows the results of three different slope which are λ= 0.33, 0.57, and 0.63 comparing with the shale rock porosity evolution trend of the North Sea and the Modified Athy's equation.

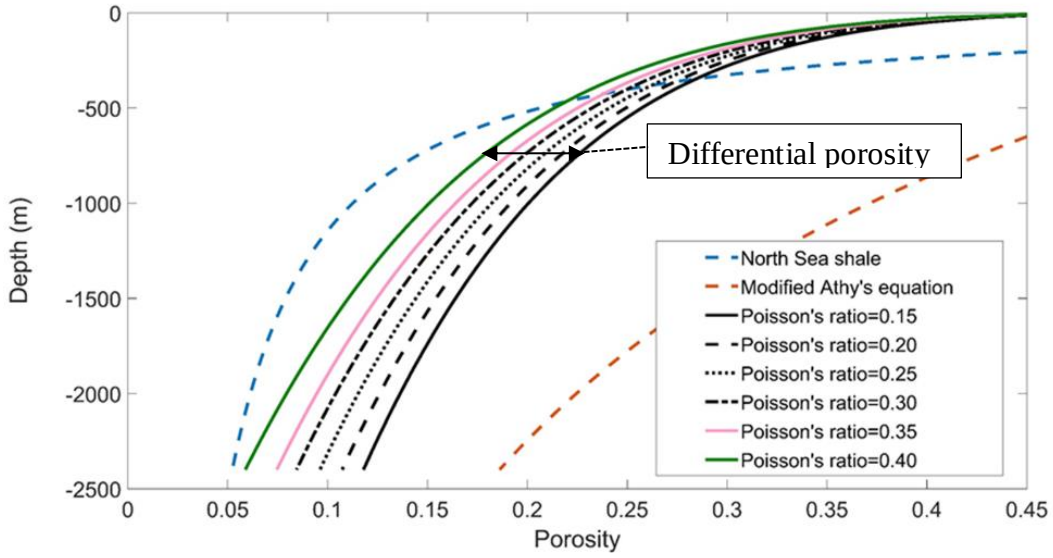

Figure 3.2. Sensitivity check of the Poisson's ratio when λ=0.57.

3.2. SENSITIVITY CHECK OF DIFFERENT PERMEABILITY AND SEDIMENTATION RATE

Overpressure occurs when the rock has low permeability, and rapid sedimentation rate and obvious overpressure are observed in a model with 1500m/m.a. sedimentation rate, composed of 100% smectite coupled Poisson's ratio evolution (Figure 3.3). Overpressure keeps developing to 16.3 MPa from the surface to 1650m and then decrease to 14.3 MPa at 2400m. The magnitude of effective stress with overpressure plus the magnitude of overpressure is the same as the effective stress without overpressure development at the same depth. The porosity is compacted normally when overpressure is not developing, and the porosity keeps constant when effect stress stops developing (e.g., 100% smectite model 0-200m). The magnitude of effective stress indicates the porosity at the same depth, and the higher effective stress will generate lower porous space.

MCCM associating with subroutine has the ability to simulate rock compaction with pore pressure development. Under physical compaction dominant environment, the degree of rock compaction is controlled by the bulk modulus affected by slope of normal consolidation and unloading/reloading lines (λ/κ) and the Poisson's ratio. Poisson's ratio has less influence on bulk modulus than λ/κ.

3.3. CASE STUDY I: THE NORTH SEA POROSITY REPRODUCE

A subroutine containing Poisson's ratio evolution from 0.5 to 0.2 is applied to this model with λ=0.57 and κ=0.19. The Poisson's ratio follows the developing trend in figure 3.4, and it generates a good matching with the North Sea porosity data. The porosity is reduced more when the subroutine is applied to the modeling process.

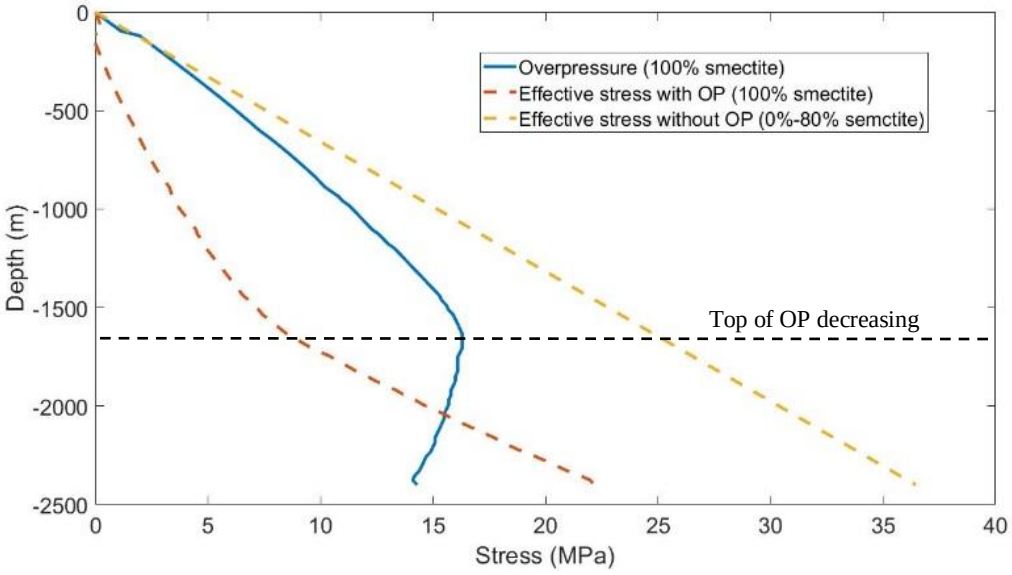

(a)

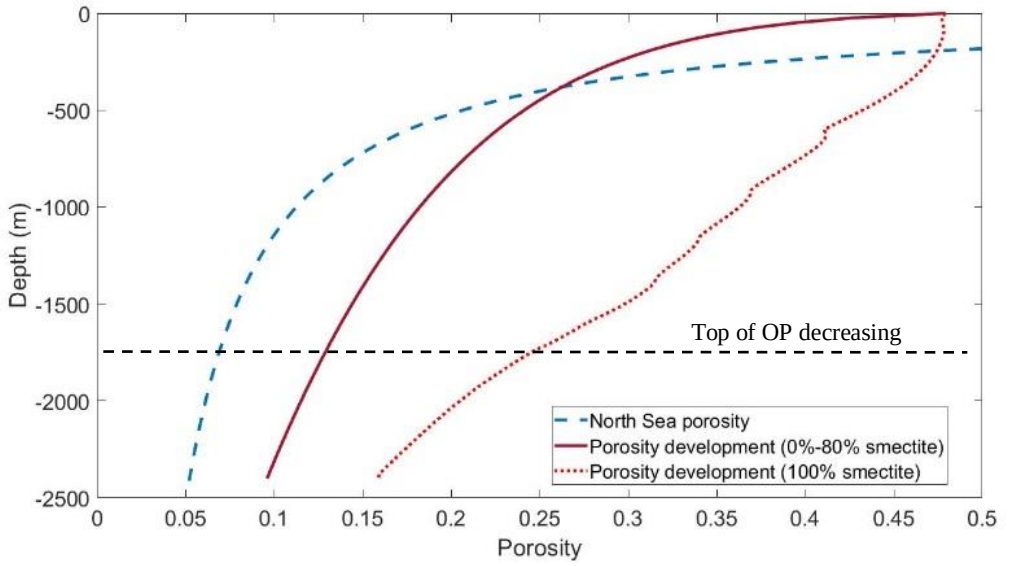

(b)

Figure 3.3. Sensitivity check of sedimentation rate and permeability. (a) Pore pressure development trends in different model initial properties; (b) porosity evolution trends related to same models of (a).

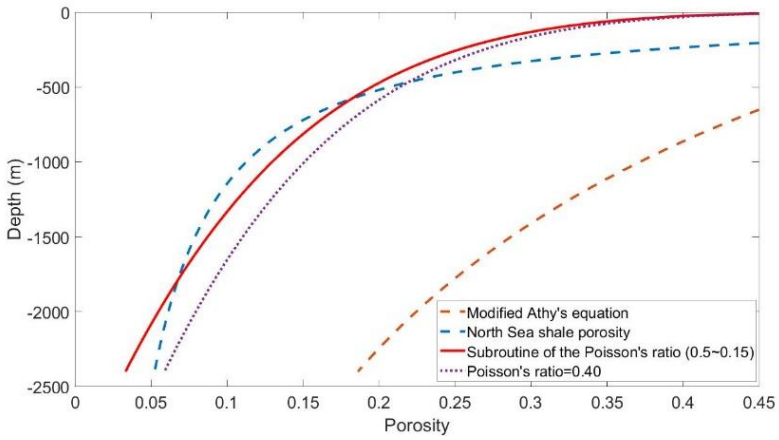

Figure 3.4. Case study I: Data reproduce of the porosity normal compaction evolution of the North Sea.

3.4. CASE STUDY II: POROSITY AND OVERPRESSURE REPRODUCE OF MINIBASIN OF THE GULF OF MEXICO

To reproduce the evolution of porosity and pore pressure of a well from the Minibasin, a 820m thick rock formation is built to simulate the compaction from surface to 2250 depth. According to the geological background, the overpressure zone has two types of rock that are sandstone containing clay minerals from 1430m to 2020m and shale rock from 2020m to 2250m. The permeability is decreasing from 1430m to 2250m, and the porosity-permeability relationship is unknown. Following Mesri and Olson (1970), several empirical functions between porosity and permeability are assigned to the subroutine to simulate overpressure development and 80% smectite-20% kaolinite permeability in sandstone layer and 100% smectite permeability in shale layer can reproduce well data well. A subroutine simulates Poisson's ratio development from 0.5 to 0.2 is also assigned to simulate rock compaction. The sedimentation rate applied above is 1200m/m.a. based on Revil and Cathles (1999) report and λ=0.42 and κ=0.14 are used.

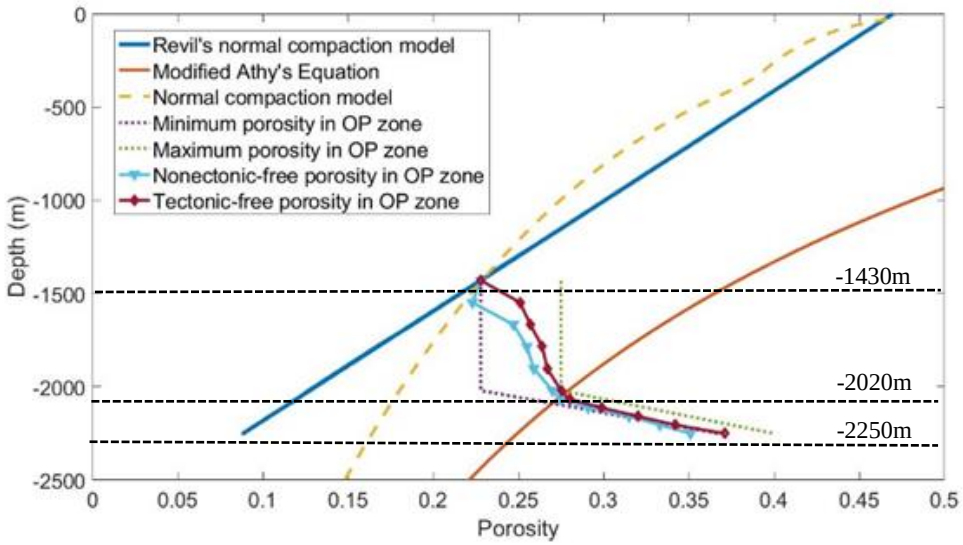

(a)

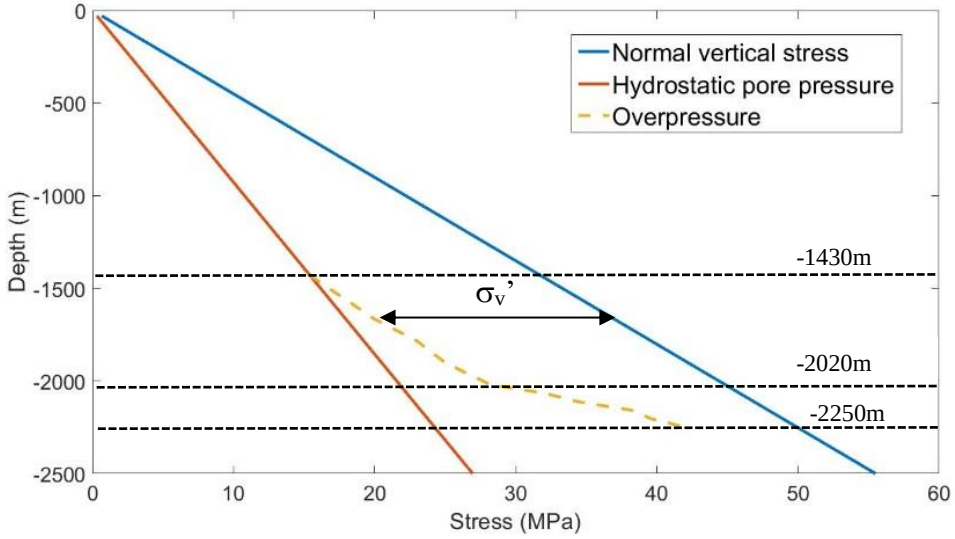

(b)

Figure 3.5. Case Study II: Field data reproduce of one well at the Minibasin of the Gulf of Mexico.

The modified Athy's equation cannot reproduce normal compaction evolution trend, and the normal compaction model has a little difference between Revil and Cathles' (1999) linear porosity development. The porosity development trend when overpressure occurs falls in the interpreted maximum-minimum porosity zone. The magnitude of

overpressure is well reproduced comparing with repeat formation testing data, and the overpressure increases faster in shale zone. The effective stress from 1430m to 2020m decreases slightly and significantly decreases in the shale zone. When the state of stress is under SH>Sh>SV regime, the porosity is slightly smaller than the tectonic-free condition with the same magnitude of overpressure.

4. DISCUSSION

Most sedimentary basin models introduce pore pressure as a constant initial condition estimated from porosity-effective stress relationship or measured directly from repeat formation test. Revil and Cathles' work (1999) introduces a detailed reservoir study about porosity and pore pressure profile at the Minibasin of Gulf Mexico. Porosity-effective stress relationship is used as the original estimation equation to derive abnormal porosity when overpressure occurs. This method can reproduce porosity very well because pore pressure is obtained from repeat formation test and the porosity and pore pressure profile are usually similar in a block area. By using this method, the whole picture of a reservoir can be drawn from one or several wild wells radially. However, a well-developed sedimentary basin model based on a specific field area cannot be applied to other basins because of different reservoir conditions (i.e., Modified Athy's equation cannot accurately reproduce porosity profile for all reservoirs such as the North Sea and Minibasin porosity profile, and it needs adjusting based on local reservoir conditions).

This study uses the Modified Cam-Clay model coupled with poroelasticity to simulate shale rock consolidation associating with pore pressure development through geological timescale. Bulk modulus, Poisson's ratio, permeability, and sedimentation rates are tested parameters influencing porosity and pore pressure development. The results show the capability of this model on porosity and pore pressure development prediction with or without tectonic stress. It shows a method that predicting porosity magnitude without introducing pore pressure as a constant boundary condition and the geomechanical model can develop pore pressure itself under physical compaction dominant environment. Other physical parameters evolution such as elastic properties and permeability are coupled

into the sedimentary basin models to improve the accuracy of pore pressure and porosity simulation. The most significant limitation of this model is that it does not consider reproducing chemical compaction and the results of this model can be less accurate if rock elastic properties and porosity-permeability relationships are unavailable. When burial history and rock physical properties are available, it can provide better reproduce of porosity and pore pressure development history.

5. CONCLUSIONS

MCCM associating with subroutine has the ability to simulate rock compaction with pore pressure development. Under physical compaction dominant environment, the degree of rock compaction is controlled by the bulk modulus affected by slope of normal consolidation and unloading/reloading lines (λ/κ) and the Poisson's ratio. Poisson's ratio has less influence on bulk modulus than λ/κ. Overpressure is built up because of rapid sedimentation rate and low permeability, and this study shows under 1500m/m.a sedimentation rate (which is very fast in nature) significant overpressure develops in 100% smectite rock (e.g. 1e-21 m^2). These mechanisms have been investigated through numerical modeling and experimental method in other researches, and MCCM can simulate rock compaction comparing with others work. The application of subroutine means to couple rock properties evolution during compaction but not to assume constant rock initial properties. This approach generates better field data reproducing results than only using constant rock properties and introducing pore pressure as an initial boundary condition. It offers a method to simulate rock compaction in pre-pressured and pre-stressed condition, and the result of it can be used to predict pore pressure and porosity evolution without drilling one or several wild wells if the sedimentary history, rock properties are known.

6. FUTURE WORK

This numerical model can reproduce rock consolidation associating with pore pressure development when physical compaction is dominant (above 3km normally). Introducing chemical compaction into modeling can be a great project in future because more complex coupling mechanisms should be included based on mineralogical change and temperature distribution. Overpressure can develop with fluid expansion caused by thermal expansion and gas generation. In forwards work, fluid expansion is also an important influence fact requiring sensitivity consideration.

APPENDIX

1. INTRODUCTION

Sedimentation rock forms due to continuously cumulative overburden pressure in sedimentation environment. During the sedimentation consolidation, different porosities and permeability are generated under various sedimentation rates and sedimentation environment. Overpressure zone development in sedimentation environment is affected by permeability of rocks and sedimentation rates primarily. A high sedimentation rate indicates a high rapid increase of overburden pressure. Permeability can be influenced by the change of overburden pressure and porosity. Permeability decreases with the increasing of overburden pressure or the decreasing of porosity.

1.1. ROCK DENSITY

Rock density is defined as mass per unit volume. Because rock is kind of porous material different porosities can be assigned to one type of rock. Rock grain density (ρ_g), is common density for describing rock density. It is defined as the ratio of total mass of rock (Mt) without pores space to the total volume (V_t):

$$\rho_b = \frac{M_t}{V_t}$$

Dry density (ρ_d) is defined as the density of the rock at the same volume without either fluid or air in the material. The relationship between dry density and bulk density is given as (Chapman, 1983) where ρ_f density of formation fluid is and $\emptyset$ is porosity.

$$\rho_b = (1 - \emptyset)\, \rho_b + \emptyset \rho_f$$

1.2. ROCK POROSITY

Porosity (∅) is the ratio of porous volume to total volume. In this study void ratio is used to describe porosity:

$$e = \frac{\emptyset}{1 - \emptyset}$$

where e is void ratio. Porosity is classified into two types as effective and ineffective porosity. The effective porosity represents ratio of interconnected porous volume to total volume. Fluid can only flow in interconnected porous space.

1.3. ROCK PERMEABILITY

Rock permeability represents the ability of a certain type of rock to allow fluid to flow through interconnected porous space. In numerical modeling method permeability is defined as (Jaeger et al., 2004):

$$k = \frac{Kg}{v}$$

where k is hydraulic conductivity (m/s) used as the input if the numerical model, K is permeability (m^2), g is the gravitational accelerator and commonly used as a constant (9.8m/s^2), and v is kinematic viscosity of the formation fluids

1.4. STRESS

A rock surface can be indicated by unit normal vector of it. Force acts on that surface can be represented by a force vector ($\vec{F}$). The traction on this surface can be defined by its traction vector ($\vec{T}$):

$$\vec{T}(\vec{n}) = \frac{\vec{F}}{A}$$

the traction vector ($\vec{T}$) over a point on the surface can be defined by limiting the surface area A to infinitesimal:

$$\vec{T}(\vec{n}) = \lim_{dA \to 0} \frac{1}{dA} d\vec{F}$$

Stress is an infinite parameter which can be defined as:

$$\vec{\sigma} = \frac{\vec{F}}{A}$$

The SI unit of stress is the Pascal (1Pa=1N/m^2).

State of stress is defined as the total result of all traction vectors through all the surfaces at a common point. The Cauchy stress tensor is able to represent state of stress at a point in the 2-D. The stress tensor can be expressed as:

$$\sigma = \begin{bmatrix} \sigma_{xy} & \tau_{xy} \\ \tau_{yx} & \sigma_{yy} \end{bmatrix}$$

The subscripts i and j can be any of x and y, representing x and y axis respectively. i is the axis that is normal to the surface. j represents the direction of the stress component. σ_{ij} is the normal stress acting perpendicular to a surface, and $\sigma_{ij}$is the shear stress acting on a surface. The stress tensor on any static point must be a symmetric matrix. τ_{xy} and τ_{yx} has the same magnitude. State of stress at a point are given by Cauchy's 2nd law:

$$T_i = \sigma_{ij} * n_j$$

where T_i and σ_{ij} are the stress tensor and the traction vector on a plane. n_j is the vector of this plane. This equation can be written in matrix form:

$$\begin{bmatrix} T_x \\ T_y \end{bmatrix} = \begin{bmatrix} \sigma_{xx} & \tau_{xy} \\ \tau_{yx} & \sigma_{yy} \end{bmatrix} \begin{bmatrix} n_x \\ n_y \end{bmatrix}$$

1.5. PRINCIPAL STRESSES

In a 2-D coordinate system when all shear are zero in magnitude a common stress can be represented by two principal stresses in principal orientations:

$$\sigma = \begin{bmatrix} \sigma_1 & 0 \\ 0 & \sigma_2 \end{bmatrix}$$

$\sigma_1$and σ_2 is principal stress.

1.6. ELASTICITY

Elasticity is the tendency of solid materials to recover to their original shape after being deformed by either internal or external forces (Jaeger et al., 2007). Linear elasticity is the most fundamental and widely-used form of elasticity. Linear elasticity is described by the general Hooke's law:

$$\sigma_{ij} = C_{ijkl}\varepsilon_{kl}$$

C_{ijkl} is elasticity matrix representing how the rock response to stresses. i, j, k may take x and y direction. The elasticity matrix contains the elastic constants such as the Young's modulus, E, and the Poisson's ratio, ν. The Young's modulus measures the axial stiffness of a linear elastic material under a load as stress per area that is needed to compress or stretch a rock sample (Jaeger et al., 2004). The SI unit of Young's Modulus is Pascal or Pa. It needs to be noted that the linear relationship between stress and strain, in general, is

only valid when the deformation is very small. The Poisson's ratio (v) is defined as the negative ratio of lateral strain to longitudinal strain. Poisson's ration can be defined as:

$$v_{ij} = -\frac{\varepsilon_i}{\varepsilon_j}$$

For isotropic rock, Young's Modulus and Poisson's Ratio can be considered as homogenous. Thus, linear elasticity can be defined as:

$$\begin{bmatrix}\sigma_{xx}\\ \sigma_{yy}\\ \sigma_{zz}\\ \sigma_{yz}\\ \sigma_{zx}\\ \sigma_{xy}\end{bmatrix} = \frac{E}{(1+v)(1-2v)}\begin{bmatrix}1-v & v & v & 0 & 0 & 0\\ v & 1-v & v & 0 & 0 & 0\\ v & v & 1-v & 0 & 0 & 0\\ 0 & 0 & 0 & 1-2v & 0 & 0\\ 0 & 0 & 0 & 0 & 1-2v & 0\\ 0 & 0 & 0 & 0 & 0 & 1-2v\end{bmatrix}\begin{bmatrix}\varepsilon_{xx}\\ \varepsilon_{yy}\\ \varepsilon_{zz}\\ \varepsilon_{yz}\\ \varepsilon_{zx}\\ \varepsilon_{xy}\end{bmatrix}$$

According to plane strain that ε_3 is zero, $\varepsilon_1$and ε_2 are nonzero

The inverse form of Hooke's law for plane strain is:

$$\varepsilon_1 = \frac{1-v^2}{E}\sigma_1 - \frac{v*(1+v)}{E}\sigma_2$$

$$\varepsilon_2 = \frac{1-v^2}{E}\sigma_2 - \frac{v*(1+v)}{E}\sigma_1$$

where σ_3 is minimum principal stress, σ_1 is maximum principal stress, σ_2 is median principal stress, and v is Poisson ratio.

1.7. ROCK BULK MODULUS

Bulk modulus is defined as the ratio of the infinitesimal pressure increase to the resulting relative decrease of the volume

$$K = -\mathrm{V}\frac{dP}{dV}$$

where P is pressure, V is volume, and dP/dV represents the derivative of pressure with respect to volume. Grain has relatively high bulk modulus (K_g). Small volume changing of solid grain has influence on porosity changing. Formation fluid is also compressed during overburden pressure increment. In order to estimate the porosity changing influenced by compressing, Biot's coefficient α, and Biot-Gassmann Theory can be defined as (Jaeger et al., 2004):

$$\alpha = 1 - \frac{K_d}{K_g}$$

$$Ku = \frac{K_g + K_d(\emptyset\frac{K_g}{K_g} - \emptyset - 1)}{1 - \emptyset - \frac{K_d}{K_g} + \emptyset\frac{K_g}{K_f}}$$

where α=1 in this study, K_d is dry bulk modulus, K_g is grain bulk modulus, and K_f is fluid bulk modulus. Storativity coefficient S are expressed as (Jaeger et al., 2004):

$$S = \frac{(1 - v_u)(1 - 2v)(1 + v)\alpha^2}{3(1 - v)(v_u - v)K}$$

1.8. FORMATION FLUID FLOWING MECHANISM

2-D Darcy' s law is introduced to describe a relationship between the flux vector q, permeability, viscosity, and the pore pressure. 2-D Darcy' s law can be described as:

$$\begin{bmatrix} q_{x\prime} \\ q_{y\prime} \end{bmatrix} = -\frac{1}{\mu}\begin{bmatrix} k_{x'x'} & 0 \\ 0 & k_{y'y'} \end{bmatrix}\begin{bmatrix} \frac{\partial P_p}{\partial x'} \\ \frac{\partial P_p}{\partial y'} \end{bmatrix}$$

where $q_{i'}$is the flow rate (m^3/s) in i axis and i may take x and y direction, $k_{i'i'}$ is the permeability (m^2) in i surface with i axis and i may take x and y direction, μ is viscosity (Pa*s) of fluids, $\frac{\partial P_p}{\partial i'}$ is pore pressure in x axis and i may take x and y direction.

1.9. EFFECTIVE STRESS

Effective stress is define as the total stress minus pore pressure. For three principal stresses, the relationship between total stresses and effective stresses are shown below:

$$\sigma_1' = \sigma_1 - \alpha P_p$$

$$\sigma_2' = \sigma_2 - \alpha P_p$$

$$\sigma_3' = \sigma_3 - \alpha P_p$$

where σ_1, σ_2, and σ_3 are total principal stresses, σ_1', σ_2', and σ_3' are effective stresses, and α is Bios's coefficient. In this study α is zero.

BIBLIOGRAPHY

Becker, S. P., Eichhubl, P., Laubach, S. E., Reed, R. M., Lander, R. H., & Bodnar, R. J. (2010). A 48 my history of fracture opening, temperature, and fluid pressure: Cretaceous Travis Peak Formation, East Texas basin. *Bulletin*, *122*(7-8), 1081-1093.

Bjørlykke, K., & Høeg, K. (1997). Effects of burial diagenesis on stresses, compaction and fluid flow in sedimentary basins. *Marine and Petroleum Geology*, *14*(3), 267-276.

Blanton, T. L., & Olson, J. E. (1997, January). Stress magnitudes from logs: effects of tectonic strains and temperature. In *SPE Annual Technical Conference and Exhibition*. Society of Petroleum Engineers.

Chang, C., Zoback, M. D., & Khaksar, A. (2006). Empirical relations between rock strength and physical properties in sedimentary rocks. *Journal of Petroleum Science and Engineering*, *51*(3-4), 223-237.

Cosgrove, J. W. (1997). Hydraulic fractures and their implications regarding the state of stress in a sedimentary sequence during burial. In *Evolution of Geological Structures in Micro-to Macro-Scales*(pp. 11-25). Springer, Dordrecht.

Goulty, N. R. (1998). Relationships between porosity and effective stress in shales. *First Break*, *16*(12), 413-149.

Hossain, M. M., Rahman, M. K., & Rahman, S. S. (2000). Hydraulic fracture initiation and propagation: roles of wellbore trajectory, perforation and stress regimes. *Journal of Petroleum Science and Engineering*, *27*(3-4), 129-149.

Kalahara, K. W. (1996, January). Estimation of in-situ stress profiles from well-logs. In *SPWLA 37th Annual Logging Symposium*. Society of Petrophysicists and Well-log Analysts.

McDermott, C., & Kolditz, O. (2006). Geomechanical model for fracture deformation under hydraulic, mechanical and thermal loads. *Hydrogeology Journal*, *14*(4), 485-498.

McLean, M. R., & Addis, M. A. (1990, January). Wellbore stability: the effect of strength criteria on mud weight recommendations. In *SPE annual technical conference and exhibition*. Society of Petroleum Engineers.

Mesri, G., & Olson, R. E. (1971). Mechanisms controlling the permeability of clays. *Clays and Clay minerals*, *19*(3), 151-158.

Mondol, N. H., Bjørlykke, K., Jahren, J., & Høeg, K. (2007). Experimental mechanical compaction of clay mineral aggregates—Changes in physical properties of mudstones during burial. *Marine and Petroleum Geology*, *24*(5), 289-311.

Moos, D., & Zoback, M. D. (1990). Utilization of observations of well bore failure to constrain the orientation and magnitude of crustal stresses: application to continental, Deep Sea Drilling Project, and Ocean Drilling Program boreholes. *Journal of Geophysical Research: Solid Earth*, *95*(B6), 9305-9325.

Olson, J. E. (2008, January). Multi-fracture propagation modeling: Applications to hydraulic fracturing in shales and tight gas sands. In *The 42nd US rock mechanics symposium (USRMS)*. American Rock Mechanics Association.

Plumb, R., Edwards, S., Pidcock, G., Lee, D., & Stacey, B. (2000, January). The mechanical earth model concept and its application to high-risk well construction projects. In *IADC/SPE Drilling Conference*. Society of Petroleum Engineers.

Prats, M. (1981). Effect of burial history on the subsurface horizontal stresses of formations having different material properties. *Society of Petroleum Engineers Journal*, *21*(06), 658-662.

Revil, A., & Cathles, L. M. (1999). Permeability of shaly sands. *Water Resources Research*, *35*(3), 651-662.

Revil, A., & Cathles, L. M. (2001). The porosity-depth pattern defined by 40 wells in Eugene Island South Addition, Block 330 Area, and its relation to pore pressure, fluid leakage, and seal migration. In *Petroleum Systems of Deep-Water Basins: Global and Gulf of Mexico Experience: Proceedings of the Gulf Coast Section Society of Economic Paleontologists and Mineralogists Foundation, 21st Annual Bob F. Perkins Research Conference* (pp. 687-712).

Sclater, J. G., & Christie, P. A. (1980). Continental stretching: An explanation of the post-mid-Cretaceous subsidence of the central North Sea basin. *Journal of Geophysical Research: Solid Earth*, *85*(B7), 3711-3739.

Steckler, M. S., & Watts, A. B. (1978). Subsidence of the Atlantic-type continental margin off New York. *Earth and planetary science letters*, *41*(1), 1-13.

Thiercelin, M. J., & Plumb, R. A. (1994). A core-based prediction of lithologic stress contrasts in east Texas formations. *SPE Formation Evaluation*, *9*(04), 251-258.

Vasseur, G., Djeran-Maigre, I., Grunberger, D., Rousset, G., Tessier, D., & Velde, B. (1995). Evolution of structural and physical parameters of clays during experimental compaction. *Marine and Petroleum Geology*, *12*(8), 941-954.

Vernik, L., Bruno, M., & Bovberg, C. (1993, December). Empirical relations between compressive strength and porosity of siliciclastic rocks. In *International journal of rock mechanics and mining sciences & geomechanics abstracts*(Vol. 30, No. 7, pp. 677-680). Pergamon.

Warpinski, N. R. (1989). Elastic and viscoelastic calculations of stresses in sedimentary basins. *SPE Formation Evaluation*, *4*(04), 522-530.

Yang, Y., & Aplin, A. C. (2010). A permeability–porosity relationship for mudstones. *Marine and Petroleum Geology*, *27*(8), 1692-1697.

Zhang, J. (2011). Pore pressure prediction from well logs: Methods, modifications, and new approaches. *Earth-Science Reviews*, *108*(1-2), 50-63.

Zhang, R., Ning, Z., Yang, F., Zhao, H., & Wang, Q. (2016). A laboratory study of the porosity-permeability relationships of shale and sandstone under effective stress. *International Journal of Rock Mechanics and Mining Sciences*, (81), 19-27.

Zhang, J. (2013). Effective stress, porosity, velocity and abnormal pore pressure prediction accounting for compaction disequilibrium and unloading. *Marine and Petroleum Geology*, *45*, 2-11.

Zhao, J., Li, J., & Xu, Z. (2018). Advances in the origin of overpressures in sedimentary basins. *Petroleum Research*, *3*(1), 1-24.

Zoback, M. D., Moos, D., Mastin, L., & Anderson, R. N. (1985). Well bore breakouts and in situ stress. *Journal of Geophysical Research: Solid Earth*, *90*(B7), 5523-5530.

Zoback, M. D. (2010). *Reservoir geomechanics*. Cambridge University Press.

VITA

Wenyu Zhao completed the first two years of his undergraduate study at the China University of Petroleum from 2012 to 2014 and attended Missouri University of Science and Technology from 2014 to 2017. He received a Bachelor of Science in petroleum engineering from Missouri University of Science and Technology in the May 2017. He started his Master's degree program in petroleum engineering in the fall of 2017, working with Dr. Andreas Eckert. In May 2019, he received his Master of Science in Petroleum Engineering from Missouri University of Science and Technology.